NIRT: Optical and Electronic Processes in Metal Nanoparticle-Conjugated Organic Materials

Cumulative Final Report

For Period June 30, 2007 - August 31, 2010

For

Prof. Theodore Goodson III
Department of Chemistry
University of Michigan

Joseph W. Perry and Seth Marder
School of Chemistry & Biochemistry
Georgia Institute of Technology
901 Atlantic Dr NW
Atlanta, GA 30332-0400
Phone: 404-385-6046
FAX: 404-385-6057
Email: joe.perry@chemistry.gatech.edu

Summary

Gold nanoparticles (*ca*. 3 nm in diameter) coated with bis(diarylamino)biphenyl-based thiols with two different alkyl spacers (propyl and dodecyl) between the chromophore and the surface-anchoring thiol group have been prepared and characterized with a variety of techniques. The excited-state dynamics of the dyes in close proximity to the nanoparticle surface were studied with the use of time-correlated single-photon counting technique and near-IR fs transient absorption spectroscopy. The excited states of the dyes in the hybrid metal / organic systems exhibit an ultrafast (<5 ps) deactivation as evidenced by the fs transient absorption measurements. The length of the alkyl spacer between the dye and the thiol group has a profound effect on the ultrafast dynamics of the photoexcited systems. An ultrafast formation (*ca.* 0.5 ps) of a cation-like species has been recorded for the system incorporating the propyl spacer but not for the dodecyl-linker system. The formation of the cation-like species has been shown to be less efficient in mixed-ligand system in which the bis(diarylamino)biphenyl-based thiol was diluted on the surface with dodecanethiol. Additionally, the ultrafast formation (*ca.* 1 ps) of a cation-like species with a similar spectroscopic signature has been observed in the solid state of the dye. A combination of the ultrafast dynamics and ^{1}H NMR spectroscopic data has been used to discuss the observed behavior in terms of dye-dye interactions in the nanoparticle systems. Due to the surface curvature of the nanoparticle, the propyl spacer imposes a closer dye-dye distance than the dodecyl spacer, thus facilitating dye-dye interactions that lead to the formation of a charge-transfer species involving two or more dye molecules.

1. Introduction

The photophysical properties of systems incorporating metal nanoparticles (NPs) have

received great attention in recent years.[1-4] Of particular interest are the effects of metal nanostructures on the dynamics of both radiative and non-radiative processes leading to depopulation of excited states of dyes placed in close proximity to the metal.[2, 4, 5] Energy and electron transfer from the photoexcited organic dye to the metal NP, as well as intermolecular interactions such as excimer formation, have been proposed as possible non-radiative channels of deactivation for excited states of dyes attached to these nanostructures.[4-9] While quenching of photoexcited fluorophores by metal NPs has already found applications,[10, 11] fundamental questions regarding the nature of the deactivation channels for excited states of molecules in close proximity to metal NPs have not yet been comprehensively answered. According to a review by Thomas and Kamat, there are three major possible deactivation channels in systems incorporating metal NPs coated with organic fluorophores.[4] The first and the most heavily studied deactivation channel involves energy transfer from a photoexcited fluorophore to the NP metallic core. Even though energy transfer has been demonstrated for a variety of organic fluorophore-metal NP systems, both on a single molecule level[12-15] and for bulk solutions of NPs,[5, 7, 16-22] the understanding of the mechanisms of energy transfer is far from being complete. Another excited-state deactivation channel involves electron transfer (ET) from the photoexcited fluorophore to the metallic core.[4] There are only a few reports that claim to demonstrate photoinduced ET from dyes in close proximity to metal NPs; this process seems to be even less well-understood than energy transfer.[6, 23-25] Dye-dye interactions are a possible third deactivation channel for excited states of dyes attached to metal NPs;[4] however, reports demonstrating the role of dye-dye interactions are also scarce.[8, 23, 26]

Design of efficient functional organic dye-metal NP systems for proposed applications in, for example, nonlinear optics,[27, 28] sensing,[29, 30] or photovoltaics[25, 31] requires a comprehensive

understanding of the mechanisms of deactivation of the excited states of organic dyes in these hybrid nanostructures. Depending on the application, it may be desirable that the excited state of the dye has a sufficiently long lifetime in order to perform a certain function (e.g. charge transfer and separation in photovoltaics,[32] or light absorption in optical pulse suppression applications[33]) or, conversely, that the photoexcited dye is efficiently quenched by the metallic core of a metal NP (e.g. in fluorescence sensing[29]). A large number of parameters in such hybrid organic-metal systems can play a role in the dynamics of different deactivation mechanisms for excited states of organic dyes:[2, 5, 15] NP size, dye orientation, dye-NP distance, and surface density of the dyes (i.e. dye-dye distance). Additionally, studying the photophysics of organic luminophores attached to the surface of metal NPs can be somewhat challenging as luminescence quenching by NP metallic cores is often very efficient.[5, 7, 34] This, in turn, results in weak luminescence signals originating from the surface-bound molecules and so unquenched luminescence exhibited by trace amounts of free dyes in solution can dominate the measured signal, as has been observed in some cases.[5,34]

We set out to investigate in detail the effect of the proximity of the nanoparticle on the excited state dynamics of one chromophore, bis(diarylamino)biphenyl (TPD). Systems incorporating gold nanoparticles with TPD moieties linked to the NP surface via a thiol group (see Figure 1) have thus been prepared and characterized with a variety of techniques. The choice of the chromophore was based mainly on two considerations. First, TPD is known to exhibit sizeable fluorescence quantum yield (0.7 in toluene solution)[35] and an emission band with significant overlap with the absorption spectrum of the Au NPs, which makes the molecule an interesting candidate for studying the energy transfer from the photoexcited dye to the metallic core of a Au NP. Second, the chromophore is characterized by a rather low oxidation potential

(+0.26 V vs $FeCp_2^+$ / $FeCp_2$ in CH_2Cl_2) and, thus, is a potentially good electron donor in electron-transfer reactions.[36] This could be relevant when studying whether any photoinduced electron transfer occurs from the photoexcited dye covalently bound to the surface to the metallic core of the Au NP.[4] Here we report on a fs transient absorption (TA) spectroscopy study addressing the influence of the linker length between a gold NP and a TPD moiety on the excited-state deactivation dynamics of the chromophore. The experimental findings yield new insight into the dynamics of excited-state deactivation of this type of organic dye. In particular, our results show clearly that dye-dye interactions play an important role in these dynamics.

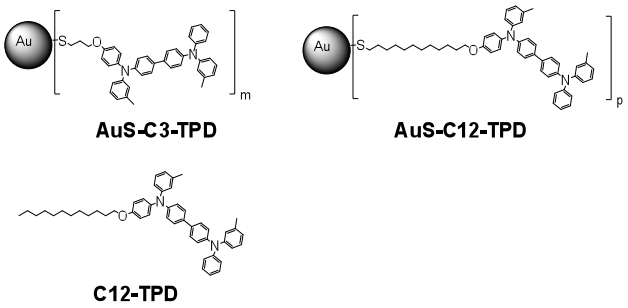

Fig. 1 Schematic structures of systems studied in this article.

2. Experimental

2.1 General

All solvents and reagents were purchased and were used without further purification with the exception of THF and toluene, which were dried by passing through columns of activated alumina in a manner similar to that described in the literature.[37] Toluene used for the preparation of solutions of gold NPs was purchased from Aldrich (spectroscopic grade) and purified in order to remove sulfur-containing impurities according to a standard procedure.[38] The **TPD-Cx-thiol** ligands, the model compound **C12-TPD**, and ligand-coated gold NPs were synthesized.

Absorption spectra were recorded on a Varian Cary 5E UV-Vis-NIR spectrometer. The fluorescence spectrum of a toluene solution of **C12-TPD** was acquired on a Fluorolog 3 fluorometer from Horiba Jobin Yvon and was corrected for the instrument response.

2.2 FT-IR analysis

Neat films of Au NPs and of **C12-TPD** were cast onto a NaCl disk from $CDCl_3$ solutions. FT-IR spectra of the films were acquired with a Perkin Elmer Spectrum 1000 spectrometer, collecting 32 scans per sample at a 4 cm^{-1} resolution. The spectrum of a clean NaCl disk was used as a reference. A spline function baseline correction, included in the instrument's software, was used to correct the baseline.

2.3 NMR analysis

NMR spectra were recorded using Bruker DRX-500, Bruker AM-250, or Varian Gemini-300 spectrometers. Measurements of ^1H NMR T_1 and T_2 relaxation times of $CDCl_3$ solutions of Au NPs were performed on a Bruker DRX-500 spectrometer. T_1 relaxation time measurements were performed using the conventional population-inversion recovery method, and the Carr-Purcell-Meiboom-Gill (CPMG) pulse sequence was employed in T_2 relaxation time measurements.

2.4 Femtosecond Transient Absorption Measurements

Femtosecond transient absorption spectra were acquired using a commercially available transient absorption spectroscopy system (Newport, Helios). This system accepts two input laser beams, one of variable wavelength used as the pump beam and one of a fixed wavelength (800

nm) used to generate the probe beam in a proprietary nonlinear optical crystal. For the pump beam, the light source was the frequency-doubled (using a BBO crystal) output of an ultrafast optical parametric amplifier (Newport, TOPAS) running at a repetition rate of 1 kHz, set to 700 nm, and pumped by a Ti:Sapphire regenerative amplifier (Newport, Spitfire), resulting in an excitation wavelength of 350 nm. The pulse width was approximately 120 fs (FWHM). The excitation wavelength is close to the lowest-energy absorption band maximum of the TPD moiety (see Figure 6). Approximately 5% of the Spitfire fundamental at 800 nm was used for NIR white-light continuum (WLC) generation (850 – 1650 nm) in the Helios nonlinear crystal to provide the experimental probe beam. The polarization of the excitation beam was set to the magic angle with respect to the polarization of the probe beam in order to sample pure depopulation dynamics. With these specifications, the instrument response function was approximately 300 – 400 fs (FWHM). The width of the temporal window that can be studied is 3200 ps. At each temporal delay point, data were averaged for 4 s. The Helios pump beam was chopped at 500 Hz to obtain pumped (signal) and non-pumped (reference) absorption spectra of the sample. The data were stored as 3-D Wavelength-Time-Absorbance matrices, which were exported for use with the fitting software. No appreciable temporal chirp of the WLC probe was observed and therefore chirp correction of the acquired transient spectra was unnecessary.

The studied solutions had OD at 350 nm between 3 and 4 in a 2 mm path length cuvette, and were stirred continuously throughout the data acquisition. A neat film of **C12-TPD** was prepared by drop casting from a toluene solution. Slow solvent evaporation resulted in a film of very good optical quality. All samples were photostable under the applied excitation conditions (no change of the transient signal was observed after ca. 10 min of signal acquisition). Average powers of 2.1 mW, 1.1 mW and 0.4 mW for the excitation beam at the sample were used for the

measurements on the NP solutions, a 0.1 M toluene solution of **C12-TPD**, and the neat film of **C12-TPD**, respectively. The excitation beam spot size at the sample was determined to be 310 μm (HW1/e). In order to avoid instrument response-related artifacts, the usable temporal delay range for single wavelength kinetic traces was determined to begin about one width of the instrument response function (or ~350 fs) after the rising edge of the signal. This point was defined as zero delay time for all fitting procedures. In general, the transient kinetic signal response for metallic NPs can be quite strong in the spectral region close to that of the surface-plasmon absorption band.[3, 39] However, due to the large spectral separation between the Au NP surface-plasmon band (ca. 520 nm) and the NIR probe wavelengths used here, only a small contribution to the overall transient ΔOD signals in the samples containing Au NPs originates from the metallic core of the NPs.

3. Results

3.1 Synthesis

Figure 2 shows the synthetic scheme for the preparation of the thiol-coated Au NPs. The NPs were synthesized by the reduction of $HAuCl_4$ in the presence of oleylamine (OA).[40] OA-coated Au NPs were then reacted in toluene with the TPD thiols with varying alkyl spacer lengths (C3 and C12), resulting in particles with high coverages of TPD thiols (**AuS-C3-TPD** and **AuS-C12-TPD** in Figure 1). Au NPs coated with dodecanethiol (DDT) were also prepared (**AuS-C12**, Figure 2), as well as Au NPs coated with mixtures of TPD-thiols and DDT (**AuS-Cx-TPD(DDT$_{60}$)**, Figure 2); these were synthesized by reacting OA-coated Au NPs with DDT or a mixture of two thiols of choice, respectively, in toluene solution. All of the prepared NPs were rather small (*ca.* 3.5 nm in diameter) and showed similar size distributions as evidenced by TEM analysis.

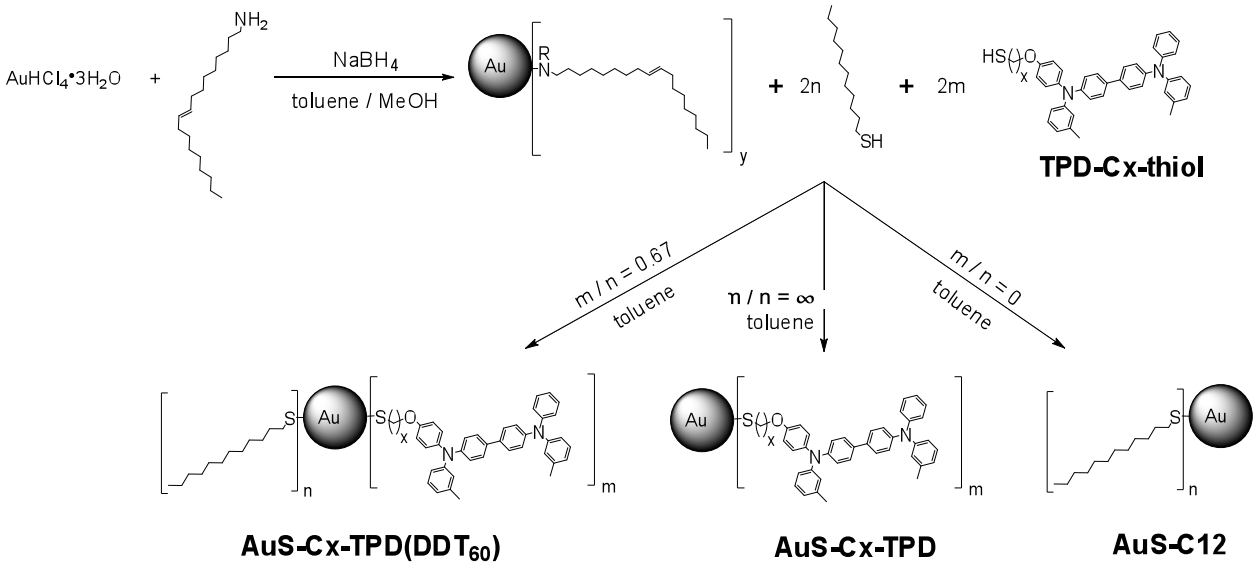

Fig. 2 Synthetic schemes for the preparation of Au NP systems coated with TPD-Cx-thiols (**AuS-Cx-TPD**), Au NP systems coated with mixtures of ca. 40% of a TPD-Cx-thiol and 60% of DDT (**AuS-Cx-TPD(DDT$_{60}$)**) and of Au NPs coated with DDT only (**AuS-C12**).

3.2 FT-IR Analysis

Infrared spectroscopy of Au NPs is routinely used in order to establish the composition and, to some extent, the structure of the organic ligand shell.[41-44] Figure 3a shows FT-IR spectra of neat films of **AuS-C3-TPD** and **AuS-C12-TPD** as well as the spectrum of a neat film of the model compound **C12-TPD**. The NP spectra exhibit signals due to IR modes characteristic of **C12-TPD**, thus confirming the presence of the TPD moiety on the surface of Au NPs. Analysis of FT-IR spectra of Au NPs coated with different mixtures of TPD-thiols and DDT was performed.

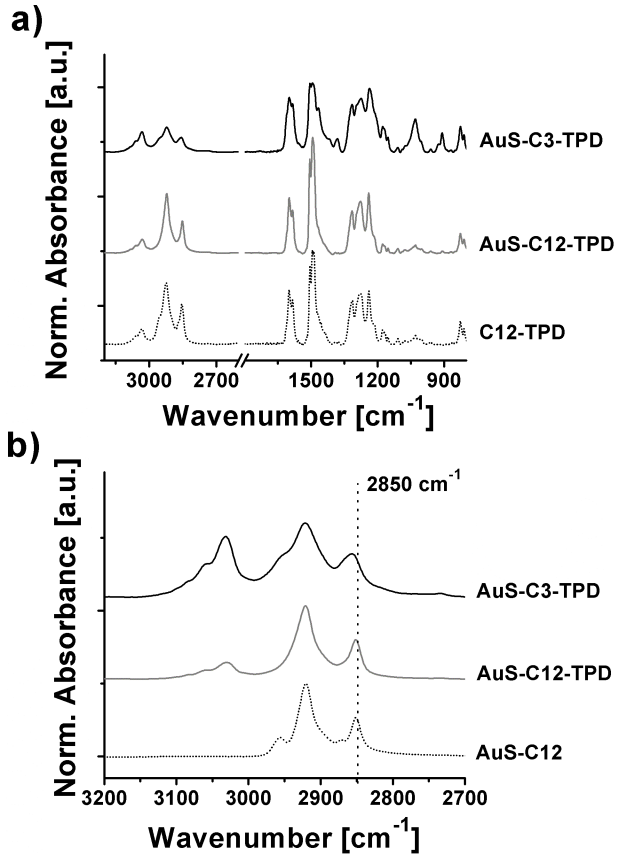

Fig. 3 a) FT-IR spectra of neat films of Au NPs coated with **TPD-Cx-thiols**, i.e. **AuS-Cx-TPD** (x = 3, 12), and of the model compound **C12-TPD**. The spectra were normalized at 1600 cm^{-1} and displaced vertically for clarity. b) FT-IR spectra of neat films of **AuS-Cx-TPD** (x = 3, 12) and of **AuS-C12** in the C-H stretching mode region. The spectra were normalized at 2920 cm^{-1} and displaced vertically for clarity.

The frequencies of the signals originating from C-H stretching modes have been often used to establish the degree of order in aliphatic chains;[44-49] in particular, it has been shown that it is possible to qualitatively establish the extent to which the all-*trans* conformation is adopted by aliphatic chains in self-assembled monolayers on flat gold surfaces and in ligand-coated Au NPs.[44, 45, 48, 49] For example, FT-IR data suggest an all-*trans* conformation of the alkyl chains in NPs coated with alkanethiols containing six or more methylene groups in the chain, with the methylene C-H symmetric stretching mode being found at 2850 cm^{-1}.[44] In NP systems incorporating shorter alkanethiols there is generally a substantial number of gauche defects,

which manifest themselves in a shift of the methylene C-H symmetric stretching mode signal to higher energy.[44] Figure 3b shows the FT-IR spectra measured for neat films of **AuS-C3-TPD** and **AuS-C12-TPD** in the spectral region of C-H stretching modes, along with a spectrum of Au NPs coated with DDT (**AuS-C12**) for comparison. As can be seen from the figure, the frequency of the signal of the methylene C-H symmetric stretching mode in **AuS-C12** is 2850 cm^{-1}, consistent with an all-*trans* conformation of the dodecanethiol chains in this system, as observed previously. A similar frequency is observed in **AuS-C12-TPD**, suggesting that in this system the alkyl linkers between the thiol group and the TPD moieties are fully extended, i.e., their conformation is dominated by the all-*trans* form.[44, 45] However, in the case of **AuS-C3-TPD** the signal of the methylene C-H symmetric stretching mode is shifted to 2858 cm^{-1}, indicative of the presence of gauche defects in the alkyl linkers between TPD moieties and the surface anchoring thiol groups, i.e., the alkyl spacers in these NPs are not fully extended. Thus, the alkyl-chain-length dependence of the extent of gauche defects, i.e. the extent of disorder, in the chains is consistent with the previously reported behavior of simple alkanethiol ligands on Au NPs mentioned above.[44] The observed behavior provides information regarding the distance between the dye and the NP surface: while in **AuS-C12-TPD** the fully extended dodecyl chain characterizes the distance between the TPD moiety and the surface-anchoring thiol group (ca. 1.6 nm), the presence of gauche defects in **AuS-C3-TPD** suggests that some of the dyes are closer to the surface than one would expect based on fully extended propyl chains (ca. 0.5 nm).

3.3 ^{1}H NMR Spectroscopic Analysis

Figure 4 shows normalized ^{1}H NMR spectra of $CDCl_3$ solutions of Au NP samples studied in this article. The presence of signals in the aryl proton region (> 6 ppm) of each

spectrum is consistent with the incorporation of TPD moieties into the NP samples. The spectra obtained for solutions of **AuS-C3-TPD** and **AuS-C12-TPD** were used to estimate the residual amount of oleylamine present in these samples (details of the calculations are given in the ESI,† page S14). The results revealed that ca. 92% of the ligand molecules in **AuS-C3-TPD** are **TPD-C3-thiol**, while the molar percentage of the corresponding thiol in **AuS-C12-TPD** system was ca. 99%. Thus it can be concluded that the amount of residual oleylamine is below 10% in both **AuS-C3-TPD** and **AuS-C12-TPD**.

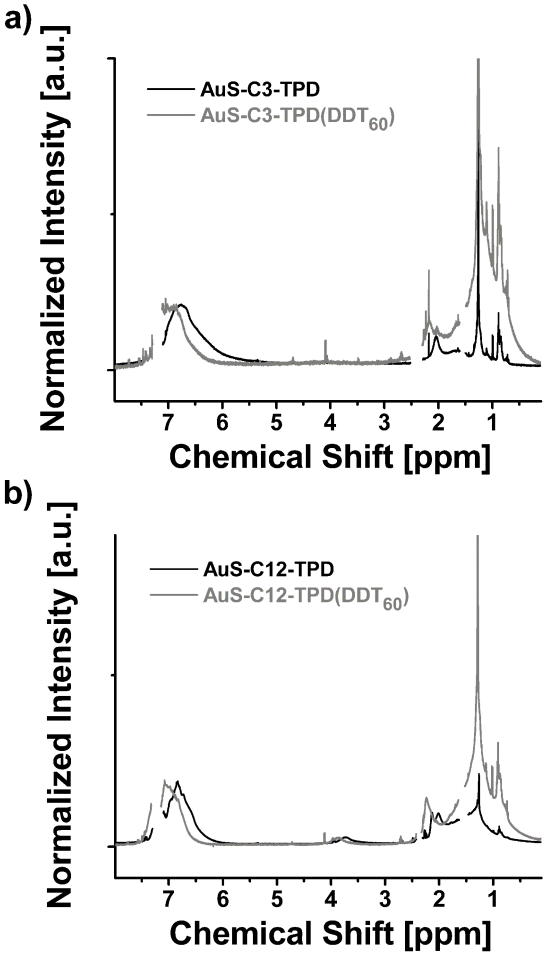

Fig. 4 ^{1}H NMR spectra of $CDCl_3$ solutions of a) Au NPs incorporating **TPD-C3-thiol**, with and without DDT and of b) Au NPs incorporating **TPD-C12-thiol**, with and without DDT. All spectra were normalized at the highest peak in the aryl-proton region (6 – 8 ppm). The residual $CHCl_3$, toluene solvent and water peaks have been masked out.

As can be seen in Figure 4, the signal intensity in the aliphatic-proton region (< 4 ppm) of the normalized ^{1}H NMR spectra is much higher for the samples prepared with mixtures of **TPD-Cx-thiol** and DDT, suggesting that using mixtures of thiols in the synthesis did indeed yield mixed-ligand systems. There is also an obvious downfield shift (towards larger chemical shift) of the aryl proton signals in the case of mixed-ligand systems (**AuS-Cx-TPD(DDT$_{60}$)**) when compared to **AuS-Cx-TPD** systems. This is true for both linker lengths and suggests that there is less shielding of aryl protons caused by ring currents of proximal arene rings[50] (i.e., by neighboring dye molecules) in the case of mixed-ligand systems. The observation of a dilution effect suggests that the distribution of **TPD-Cx-thiol** and DDT on the surface of NPs is roughly statistical, rather than consisting of phase-segregated domains (i.e., consisting of patches of **TPD-Cx-thiol** and DDT).

The broadness of the signals seen in the ^{1}H NMR spectra of the NP systems studied here is expected for ligands attached to the surface of Au NPs;[51-53] previously both inhomogenous broadening, arising from a distribution of chemical shifts caused by different adsorption sites on the NP surface,[51, 54-56] and a drastic shortening of the spin-spin relaxation time, T_2,[54, 55, 57] caused by the increased viscosity of the microenvironment close to the surface of a NP,[51, 55] have been found to contribute to the broadness of ^{1}H and ^{13}C NMR signals of NP-bound ligands. Moreover, the fact that sharp signals of unbound **TPD-Cx-thiols** are essentially undetectable suggests that the vast majority of TPD moieties present in the studied samples are, in fact, attached to the NP surface. Measurements of spin-spin relaxation times (T_2) for **AuS-C3-TPD** and **AuS-C12-TPD**[1] confirm that a shortening of T_2 is a major contributor to broadening of the ^{1}H signals in

[1] The spin-spin relaxation time measurements were performed on a different batch of **AuS-Cx-TPD** (x = 3, 12) from the batch discussed in the rest of this paper. The average diameters of the second batch of these NPs were found from TEM analysis to be 2.8 ± 0.8 nm and 3.2 ± 0.7 nm for **AuS-C3-TPD** and **AuS-C12-TPD**, respectively.

these samples; Figures 5a and 5b show decays of proton signals for **AuS-C3-TPD** and **AuS-C12-TPD** measured in the Carr-Purcell-Meiboom-Gill (CPMG) experiment for two different spectral regions – 2.05 ppm corresponds to the chemical shift of the methyl protons in tolyl groups of the TPD moiety, and 6.90 ppm corresponds to the chemical shift of the aryl protons of the TPD moiety. The average T_2 relaxation times, defined as the time delay after which the signal intensity is reduced by a factor of e – presented in Figure 5c – are clearly much shorter than those found for organic molecules in solution, which are on the order of seconds.[50] Additionally, measurements of spin-lattice relaxation time, T_1, for $CDCl_3$ solution of **AuS-C3-TPD** revealed the T_1 to be on the order of seconds, which is typical for organic molecules in solution.[50] This behavior is thus consistent with a relaxation mechanism dominated by homonuclear magnetic dipole-dipole interaction,[51, 55] rather than by interactions of the protons with any paramagnetic centers that might be present in the NPs.[55]

It is interesting to note that the average T_2 values found for **AuS-C3-TPD** are significantly smaller than those found for **AuS-C12-TPD** (Figure 5c). Since

$$\frac{1}{T_2} \propto \frac{1}{R^6}\tau_c \qquad \textbf{Equation 1}$$

where R is the distance between the interacting nuclei and τ_c is the molecular motion correlation time, which is directly proportional to the viscosity of the environment,[51] this observation is consistent with higher restrictions on molecular motion in the case of the system incorporating the shorter alkyl linker between the TPD moiety and the surface-anchoring thiol group. In other words, if the dominating mechanism of T_2 relaxation in the studied NP systems is indeed the homonuclear dipole-dipole interaction, as the data suggest, the difference in T_2 measured for **AuS-C3-TPD** and **AuS-C12-TPD** can be explained by a decrease of the local viscosity of the

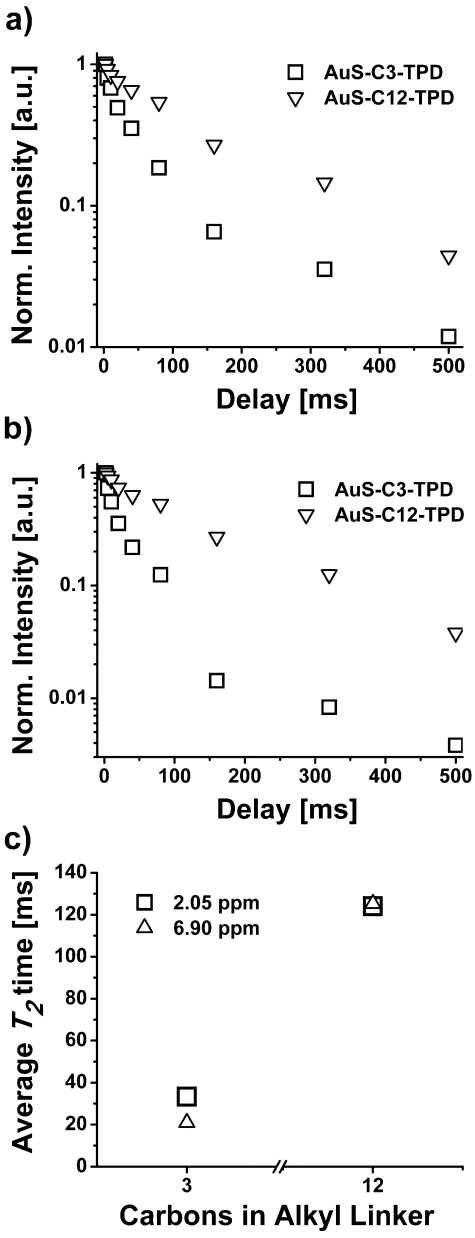

Fig. 5 Decays of ^{1}H NMR signals as a function of delay between pulses in the CPMG experiment measured at a) 2.05 ppm and b) 6.90 ppm, for $CDCl_3$ solutions of **AuS-C3-TPD** and **AuS-C12-TPD**. c) Average T_2 relaxation times found for **AuS-C3-TPD** and **AuS-C12-TPD** in $CDCl_3$ solutions.

environment in which the dyes are immersed with a subsequent increase of the proton-proton distance for the system with longer length of the alkyl linker between the thiol group and the

TPD moiety. This can be related to the geometry of **AuS-Cx-TPD** systems. Similarly to what has been reported for alkanethiol-coated Au NPs,[51] due to the surface curvature of Au NPs the molecular packing density is smaller when the TPD moiety is located further away from the NP surface, resulting in lower local viscosity and larger intermolecular proton-proton distances and, according to equation 1, leading to longer T_2 relaxation times. Thus, the T_2 data suggest that the average TPD-TPD distance is larger in **AuS-C12-TPD** than in **AuS-C3-TPD**, as expected from the idealized structures (Figure 1).

3.4 UV-Vis Absorption and Fluorescence Spectral Analysis

The electronic absorption spectra of toluene solutions of **AuS-C3-TPD**, **AuS-C12-TPD**, **AuS-C12** and of the model compound **C12-TPD** are presented in Figure 6.

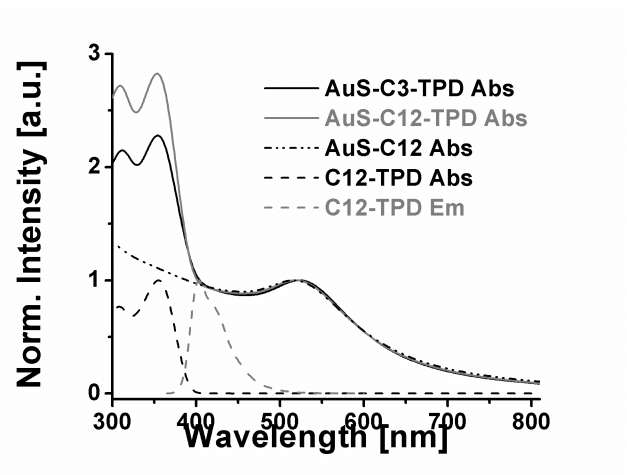

Fig. 6 UV-Vis absorption spectra (Abs) measured for toluene solutions of the systems studied herein, normalized at the lowest-energy absorption maxima. A normalized fluorescence spectrum (Em) of **C12-TPD** in toluene solution is also shown.

The absorption spectra of the NP systems exhibit the surface-plasmon resonance band (~520 nm) typically observed for Au NPs with diameters larger than 2 nm.[51, 58] Absorption spectra of both NP systems also reveal an absorption band around 350 nm, very similar to that

measured for a toluene solution of **C12-TPD**, further confirming the presence of the TPD moiety in the NP systems. The absorption spectra of the NP systems prepared with mixtures of thiols were also measured.

As can be seen in Figure 6, the fluorescence spectrum of the model compound **C12-TPD** in toluene solution exhibits a maximum at 403 nm and it overlaps primarily with the interband absorption spectrum associated with the Au core of **AuS-Cx-TPD**. Due to this spectral overlap, one can expect that in the fluorophore – NP coupled system the fluorescence will be quenched by the metallic core of the NP via energy transfer.[2, 4, 7] We initially set out to investigate the influence of the distance between the NP surface and the fluorophore on the quenching of excited state of the dye with the use of the time-correlated single-photon counting (TC-SPC) technique. Figure 7 shows fluorescence decays of toluene solutions of the free chromophore, **C12-TPD,** and of **AuS-C12-TPD**.

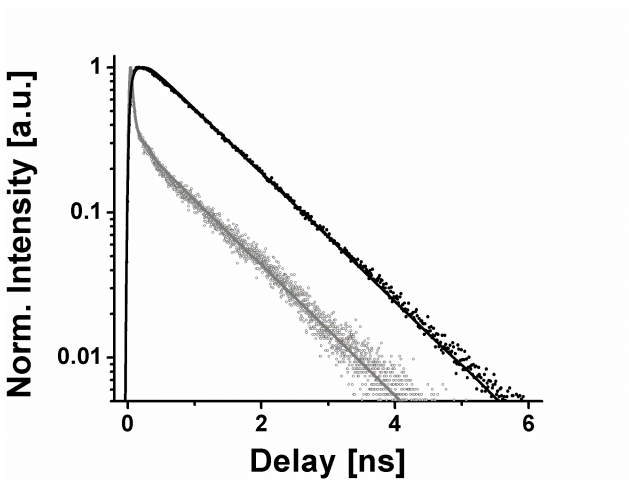

Fig. 7 Normalized fluorescence decays collected at 420 nm for air-saturated toluene solutions of **C12-TPD** (black circles) and of **AuS-C12-TPD** (gray circles) excited at 365 nm. The best-fit curves are shown as solid lines.

The analysis of the decay curve measured for a toluene solution of **C12-TPD** revealed a monoexponential decay lifetime of 0.98 ns. Interestingly, the decay recorded for **AuS-C12-TPD**

shows a somewhat similar behavior; i.e., the long-lived signal, that dominates the integrated signal, shows a comparable lifetime (ca. 0.96 ns) to that measured for the model compound **C12-TPD**. Additionally, there is a very fast component of the decay seen after photoexcitation of **AuS-C12-TPD** that dominates the zero time signal amplitude. The dynamics of the short-lived component were limited by the instrument response function (ca. 70 ps) and, thus, its lifetime could not be established. The presence of two decay components in the fluorescence decay of toluene solutions of **AuS-C12-TPD** reveals that there are at least two excited-state species present after photoexcitation of the sample. Further, the similarity between the lifetime of the long-lived component and the lifetime measured for **C12-TPD** suggests that the long-lived component seen in the fluorescence decay of photoexcited **AuS-C12-TPD** could originate from an unbound form of the dye. While **TPD-C12-thiol** and the corresponding disulfide could not be detected by a thin-layer chromatography analysis of the NP sample after its purification, presumably there is a small population (ca. 1%) of unbound TPD-based species in the NP sample solution, the fluorescence of which would be expected to be unquenched by the NP cores. The short-lived component, which constitutes only ca. 25% of the integrated fluorescence signal, most likely originates from the surface-bound TPD moieties and the short lifetime can be attributed to efficient quenching by the metallic core of the Au NPs (which is further evidenced by the fs TA measurements described in section 3.5). Effectively, the contrast in fluorescence quantum yields between the bound and unbound species results in a situation in which even a very small fraction of unbound species can give rise to a fluorescence signal that dominates the integrated fluorescence signal. Similar observations have been made by Dulkeith et al. and by Soller et al. for different fluorophore-NP systems, for which the authors assigned the observed long-lived components of the luminescence decays to emission originating from unbound

luminophores.[5, 34] While we cannot generalize such behavior for all fluorophore-NP systems, we suggest that TC-SPC analysis should be performed with caution and, especially in situations in which the measured fluorescence decay implies that there is no or very little fluorescence quenching by the NPs, additional measurements may be necessary in order to determine if the measured signal originates from surface-bound species. In our case, an additional complication was posed by the instability of the fluorescence intensity, which was observed to steadily increase during the signal acquisition. Due to the aforementioned obstacles, we turned to fs transient absorption to gain further insight into the kinetics of the excited states of the NP-bound chromophores.

3.5 Femtosecond Transient Absorption Spectroscopy

Since transient absorption (TA) signals do not depend on the fluorescence quantum yield and the presence of trace amounts of unbound dyes has negligible effects on the total signal, the issues described in the previous section do not apply. In order to address the question of the influence of the alkyl spacer between the Au NP and TPD moiety on the deactivation dynamics of the TPD excited state, we employed a fs near-infrared (NIR) broadband TA technique. The use of the NIR probe allowed for preferential probing of the photoexcited TPD moiety as the contribution from the Au NP metallic core to the overall TA signal is minor in this spectral region, as opposed to the visible region of the spectrum where the bleaching of the surface plasmon resonance band and the absorption originating from the photoexcited NPs dominate the transient spectra.[3, 39]

As presented in Figure 8, photoexcited samples of **AuS-C12-TPD** and **AuS-C3-TPD** in toluene (the excitation wavelength was 350 nm) exhibited an ultrafast decay of the TA signal.

Global fitting of the kinetic data for **AuS-C12-TPD** at different wavelengths using a biexponential function yielded one major component of the decay with a time constant of 2.4 ps and a spectral distribution identical to an early time (*ca.* 1 ps delay) transient spectrum of photoexcited **C12-TPD** in toluene solution (Figure 8d). For comparison, the excited-state lifetime of 0.1 M solution of **C12-TPD** in toluene was measured to be ca. 700 ps. Thus, the lifetime observed for the TPD excited state in **AuS-C12-TPD** is more than two orders of magnitude shorter than that for the same isolated chromophore in solution. This is most likely due to an efficient energy transfer from the photoexcited dye to the Au NP facilitated by the close proximity of the thiol-anchored TPD moiety to the NP surface, and by the significant spectral overlap of the TPD fluorescence with the absorption of the NPs (Figure 6).[7]

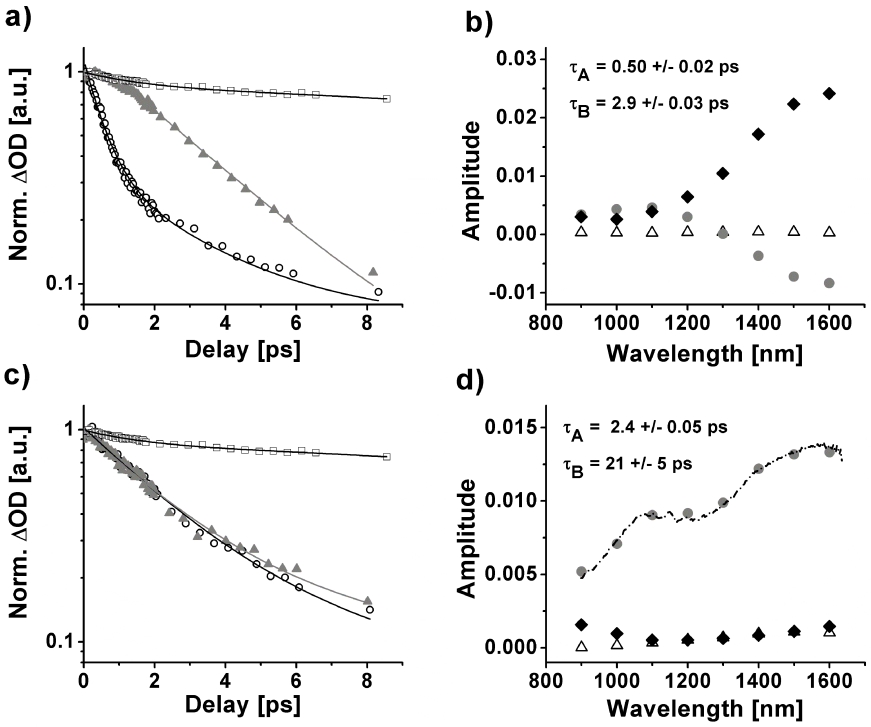

Fig. 8 Left: Normalized TA kinetic traces measured at (○) 1000 nm and (▲) 1600 nm for a toluene solution of a) **AuS-C3-TPD** and c) **AuS-C12-TPD**. The open squares represent the 1600 nm decay measured for a 0.1 M toluene solution of **C12-TPD**. The solid lines are the corresponding best-fit curves. Right: Lifetimes and spectral distributions of amplitudes (● for τ_A, ◆ for τ_B, △ for offset) obtained from global fitting of the data with a sum of two exponential

decays for b) **AuS-C3-TPD** and d) **AuS-C12-TPD**. The dash-dot line in d) shows the spectrum measured at a delay of ca. 1 ps for a 0.1 M **C12-TPD** toluene solution.

In contrast to **AuS-C12-TPD**, **AuS-C3-TPD** showed rather different excited-state decay kinetics, as presented in Figure 8a. Perhaps rather surprisingly, the overall average TA signal lifetime at 1600 nm in **AuS-C3-TPD** (τ_{av} = 3.7 ps) is larger than that observed in **AuS-C12-TPD** (τ_{av} = 2.9 ps) (ESI, Fig. S11).[†] Additionally, the shapes of the kinetic profiles measured at 1000 and 1600 nm for **AuS-C3-TPD** in toluene are clearly different, implying the presence of at least two NIR-absorbing species in the photoexcited sample. Global fitting of the data using a biexponential function provided two major decay components (Figure 8b). One of the components showed a very short lifetime of 0.5 ps (with a transient spectrum similar to that of the early time spectrum of photoexcited **C12-TPD** in Figure 8d) and a spectral distribution of preexponential amplitudes implying a growth of ΔOD values in the long wavelength region of the spectrum (negative amplitude values). The second component shows a slower decay rate (τ_B = 2.9 ps) and a spectral distribution that is complementary to that measured for the ultrafast growth. This implies that the TPD excited state in the photoexcited **AuS-C3-TPD** decays very rapidly (τ_A = 0.5 ps) resulting in the generation of a spectrally distinct species, which lives for 2.9 ps.

The striking difference in the photophysics of **AuS-C12-TPD** and **AuS-C3-TPD** is almost undoubtedly associated with the difference in the length of the alkyl spacer between the thiol group and the TPD moiety. In order to investigate whether the alkyl spacer-mediated differences in the photophysics of **AuS-C12-TPD** and **AuS-C3-TPD** are a result of dye–NP or dye–dye interactions, the mixed-ligand systems, i.e. **AuS-Cx-TPD(DDT$_{60}$)**, were analyzed in the

same way. A comparison of kinetic traces measured for **AuS-C3-TPD** with those measured for the corresponding mixed-monolayer system, **AuS-C3-TPD(DDT$_{60}$)**, is shown in Figure 9a.

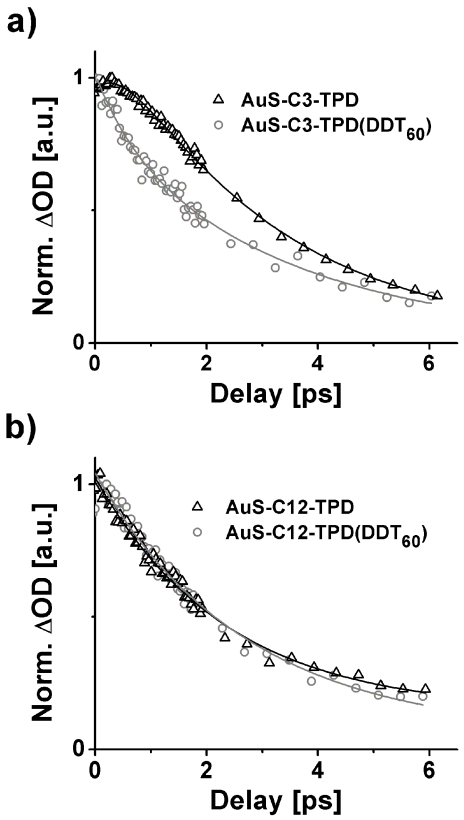

Fig. 9 Normalized TA kinetic traces measured at 1600 nm for toluene solutions of a) **AuS-C3-TPD** and **AuS-C3-TPD(DDT$_{60}$)**, and b) **AuS-C12-TPD** and **AuS-C12-TPD(DDT$_{60}$)**. The solid lines are the corresponding best-fit curves.

It is clear that diluting **TPD-C3-thiol** with DDT on the surface of Au NPs (*ca.* 40% of **TPD-C3-thiol**, see ESI page S17)[†] leads to a change in the kinetics of the photoexcited sample. In fact, the lifetime of the initially excited TPD moiety in **AuS-C3-TPD(DDT$_{60}$)** was found to be slightly longer (*ca.* 0.64 ps) than that found in **AuS-C3-TPD** (*ca.* 0.50 ps) indicating that the efficiency of the formation of the spectrally distinct species is lower in the mixed-ligand system. At the same time, no difference was observed between the decay kinetics of **AuS-C12-TPD** and the corresponding mixed monolayer system **AuS-C12-TPD(DDT$_{60}$)** (Figure 9b). These data

suggest that the process leading to the alkyl-spacer-length related differences in the photophysics involves interactions between surface-bound dyes rather than interactions between the Au NP and the dye.

The possibility that dye-dye interactions are involved in the kinetics behavior observed in **AuS-C3-TPD** prompted us to examine the photophysics of **C12-TPD** in the solid state. A neat film of **C12-TPD** was prepared and a fs TA experiment was performed. Figure 10 shows the lifetimes and spectral distributions of decay components found from a global fitting analysis performed on the decay data acquired for the neat film of **C12-TPD**.

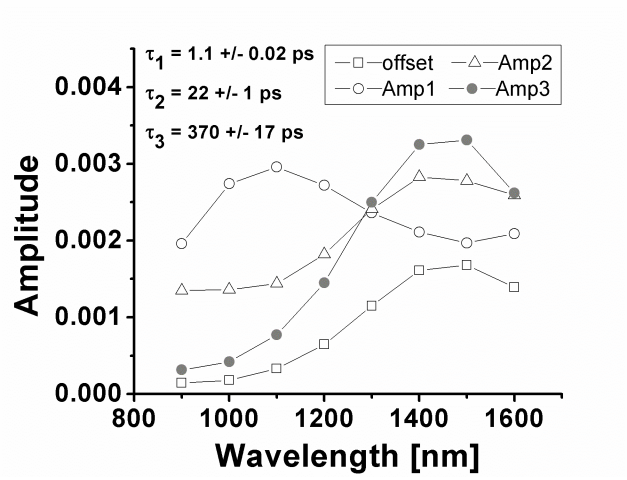

Fig. 10 Lifetimes and spectral distribution of amplitudes from global fitting of the data with a sum of three exponential decays for the neat film of **C12-TPD**.

The excited-state dynamics of **C12-TPD** in the solid state are rather complicated and show different characteristics from those seen for the 0.1 M toluene solution. The analysis of the decay components present in the photoexcited **C12-TPD** neat film reveals that the initially excited TPD moiety, which exhibits the same spectral profile as the initially-excited TPD moiety in toluene solution, decays very rapidly (τ_1 = 1.1 ps) to form a spectrally-distinct species (Amp3

and offset in Figure 10).[2] The new species exhibits two channels of deactivation – one with a lifetime of 370 ps (Amp3 in Figure 10) and one with a lifetime that is most likely longer than 10 ns (offset in Figure 10). As shown in Figure 11, the spectrum of the new species is practically the same as a steady-state absorption spectrum measured for the chemically-generated radical cation of **C12-TPD**. Moreover, the spectrum of the species photogenerated in **AuS-C3-TPD** shows a remarkable similarity to both the spectrum of the long-lived species seen in the neat film of **C12-TPD** and the spectrum of the **C12-TPD** radical cation.

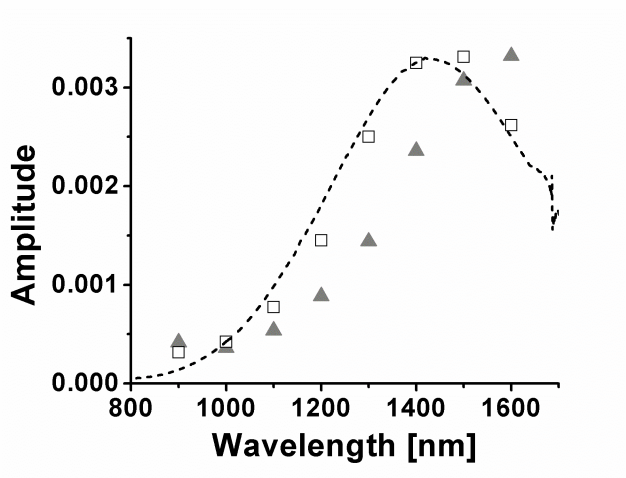

Fig. 11 Spectral distribution of the decay component with 2.9 ps lifetime present in **AuS-C3-TPD** (▲) and of one of the major decay components present in the **C12-TPD** neat film (□). The dashed line shows the absorption spectrum of chemically oxidized **C12-TPD** in toluene in the NIR region.

4. Discussion

The generation of a TPD radical cation-like species after photoexcitation found in **AuS-C3-TPD**, but not in **AuS-C12-TPD**, suggests that a photoinduced electron-transfer (ET) process

[2] The nature of the component with spectral distribution Amp2 and lifetime of 22 ps is not clear. However, it is important to note that the spectral distribution shows a peak that is similar in position to the peak that dominates the spectral distributions of the decay components of the new species (Amp3 and offset in Figure 10) as well as an appreciable amplitude in the spectral range in which the initially excited **C12-TPD** absorbs (900 nm - 1200 nm). This suggests that the 22 ps decay component is a manifestation of a fast deactivation channel of both the initially excited **C12-TPD** and of the new species, which can be interpreted as a recombination process involving a fraction of the initially excited **C12-TPD** molecules and a fraction of the population of the new species.

leading to some degree of charge separation may take place in the former system. The question arises: what is the electron acceptor in **AuS-C3-TPD**? Before we attempt to answer this question we must first turn the discussion to the photophysics of the neat film of **C12-TPD**.

As described above, the long-lived species photogenerated in the neat film of **C12-TPD** exhibits a spectral profile that is essentially the same as the spectrum of **C12-TPD** radical cation. Thus, the spectrum of the photogenerated species in the **C12-TPD** neat film can be attributed to either a **C12-TPD** radical cation or to a charge-transfer type exciton.[59, 60] Tsuboi et al. demonstrated that the efficiency of quenching of the fluorescence of TPD in a solid mixture with polystyrene was lower than in the neat film of TPD, thus suggesting that dye-dye interactions are responsible for the observed excited-state deactivation.[61] The authors attributed the quenching process to a photoinduced ET between a photoexcited TPD molecule and another TPD molecule in a ground state.[61] Our data acquired for a very similar system, **C12-TPD**, and in particular the contribution of a cation-like species to the spectrum of the photoexcited film seem to support the process of photoinduced ET between two TPD molecules as one of the mechanisms of deactivation of the initially excited state of TPD in the solid. We have not, however, independently verified whether TPD radical anion is formed in the solid, as the spectral signature of such species has not been reported in the literature. While, at present, it is impossible to state definitively whether the formation of radical cation-like species in the solid state of **C12-TPD** is due to a photoinduced ET (which would also generate a radical anion) or due to a formation of charge-transfer exciton (similar to what has been proposed for sexithiophene)[59, 62], both scenarios are consistent with deactivation of the initially-excited TPD via a channel involving dye-dye interactions with a subsequent formation of a cation-like species.

We can now return to the question posed at the beginning of this section, i.e., if

photoinduced electron-transfer (ET) takes place, what serves as the electron acceptor in **AuS-C3-TPD**? The origin of the difference in behavior in **AuS-C3-TPD** and **AuS-C12-TPD** also needs to be addressed. Based on the fs TA data, there is a clear influence of linker length on the formation of the cation-like species. While for **AuS-C3-TPD**, in which the TPD moiety is located close to the surface, there is an ultrafast formation of the cation-like species, there is no sign of this species in **AuS-C12-TPD**, in which TPD is located further away from the NP surface. This result is at least consistent with electron transfer from a photoexcited TPD moiety to the Au NP core in **AuS-C3-TPD** (i.e., with the NP core functioning as the electron acceptor), with the donor-acceptor distance in **AuS-C12-TPD** being sufficiently large that photoinduced electron transfer is too slow to compete significantly with other deactivation mechanisms.[3] However, the results obtained for mixed-ligand systems indicate that the formation of the cation-like species is less efficient in **AuS-C3-TPD(DDT$_{60}$)** than in **AuS-C3-TPD**, and strongly suggest that dye-dye interactions are involved in the formation of the species. This dye-dye interaction is also supported by the observation of cation-like species in the solid state of **C12-TPD**. Thus the different behavior of **AuS-C3-TPD** and **AuS-C12-TPD** seems not to be due to the different TPD moiety-NP distances, but to different dye-dye distances arising from the surface curvature and the linker lengths:[51] based on estimates of the lengths of the alkyl spacers (ca. 0.5 nm and 1.6 nm for fully extended C3- and C12-linkers, respectively), and the measured NP radius, the dye-dye distance is estimated to be approximately 1.5 times larger in **AuS-C12-TPD** than in **AuS-C3-TPD**[4]. This is entirely consistent with the NMR data presented in section

[3] The products of such reaction in **AuS-C3-TPD** would be the radical cation of the TPD moiety and a negatively charged core of a Au NP. Direct spectroscopic evidence for the latter would likely be difficult to discern due to small spectral changes associated with the change of the number of conduction-band electrons in Au NPs (ref. 58) and to the presence of transient signals originating from the photoexcited Au NP in the visible part of the spectrum.

[4] The calculated value of the dye-dye distance ratio was based on fully extended alkyl spacers for both **AuS-C3-TPD** and for **AuS-C12-TPD**. According to FT-IR data the alkyl spacer in **AuS-C12-TPD** is fully extended but that is not the case for **AuS-C3-TPD**. This implies that the dye-surface distance and dye-dye distance in the latter system

3.3, which suggest that the dye-dye distance in **AuS-C3-TPD** is indeed smaller than that in **AuS-C12-TPD**.

Thus, while our data do not enable us to distinguish between ET from one TPD molecule to another, which would generate a TPD radical anion[5] and TPD radical cation pair, or the formation of a charge-transfer exciton, the results strongly suggest the formation of a radical-ion like species whose formation involves dye-dye interactions rather than dye-NP interactions.

5. Conclusions

We have shown that the alkyl spacer length between a Au NP and a covalently attached organic dye has a significant impact on the resulting excited-state dynamics. This is manifested not only in the well-known dye-NP energy-transfer excited-state deactivation mechanism,[6] but also in the presence of a deactivation channel involving the formation of a radical cation-like species through dye-dye interactions. Additionally, we have shown that while fluorescence-based measurements were not feasible for studying the dynamics in these systems, the fs NIR transient absorption technique is an excellent method for probing the excited-state dynamics of TPD moieties attached to Au NPs. Furthermore, we have demonstrated that the presence of a spectral signature very similar to the radical cation of the dye in the photoexcited Au NP/dye system does not necessarily imply a photoinduced electron transfer from the dye to the metallic core of the Au NP. Rather, the demonstrated dye-coverage dependence of the photophysics and the similarity of the photophysical properties of toluene solutions of **AuS-C3-TPD** to those of **C12-**

---

are most likely smaller than the distances used in calculation of the dye-dye distance ratio. Consequently, the dye-dye distance in **AuS-C12-TPD** is most likely larger than the dye-dye distance in **AuS-C3-TPD** by a factor of >1.5.

[5] As in the case of **C12-TPD** neat film, the formation of TPD radical anion in **AuS-C3-TPD** has not been ascertained at this stage due to the lack of literature data regarding the spectral signature of such species.

[6] The dye - surface distance dependence of the energy transfer from the TPD moiety to the metallic core in the studied systems will be discussed in a separate paper.

TPD in the solid state suggest the formation of either a radical anion/radical cation pair between two dye molecules, or the formation of a charge-transfer type exciton incorporating a few dye molecules in the photoexcited nanostructure. In any case, only the NP system incorporating the short linker between the dye and the NP surface exhibits the solid-like behavior.

The novelty of our work lies not only in the use of fs NIR transient absorption, which allows for probing selectively the ultrafast dynamics of the surface-bound dyes, but also in our finding that such ultrafast dynamics provide important insights into the structure of the ground state of the hybrid NP – organic dye systems, in a similar fashion to what has been demonstrated for molecular systems.[63-65] Perhaps the most important new physical insight resulting from this work is that the surface curvature hinders dye-dye interactions for systems with long spacers between the dye and the NP surface, while the short chain system displays features that resemble those of the dye in the solid state. From a scientific standpoint the consequences of the present data are important as they clearly show that dye–dye interactions can play a significant role in the excited-state dynamics of Au NP/organic dye systems. These results could be of interest for the design of NP/organic dye hybrid systems for applications in which the lifetime of the excited state is a critical parameter.

Acknowledgement

This work was supported in part by National Science Foundation (through the NIRT Program Number DMR 0454533 and STC Program under Agreement Number DMR-0120967), and by the US Army Research Office (Grant No. 50372-CH-MUR). We would like to thank Dr. Leslie T. Gelbaum for his help with ^{1}H NMR relaxation measurements.

References

1 M. C. Daniel and D. Astruc, *Chem. Rev.*, 2004, **104**, 293-346.
2 S. K. Ghosh and T. Pal, *Phys. Chem. Chem. Phys.*, 2009, **11**, 3831-3844.
3 S. Link and M. A. El-Sayed, *Annu. Rev. Phys. Chem.*, 2003, **54**, 331-366.
4 K. G. Thomas and P. V. Kamat, *Acc. Chem. Res.*, 2003, **36**, 888-898.
5 E. Dulkeith, A. C. Morteani, T. Niedereichholz, T. A. Klar, J. Feldmann, S. A. Levi, F. C. J. M. van Veggel, D. N. Reinhoudt, M. Moller and D. I. Gittins, *Phys. Rev. Lett.*, 2002, **89**, 203002/203001-4.
6 S. Barazzouk, P. V. Kamat and S. Hotchandani, *J. Phys. Chem. B*, 2005, **109**, 716-723.
7 C. Fan, S. Wang, J. W. Hong, G. C. Bazan, K. W. Plaxco and A. J. Heeger, *Proc. Natl. Acad. Sci. U. S. A.*, 2003, **100**, 6297-6301.
8 B. I. Ipe and K. G. Thomas, *J. Phys. Chem. B*, 2004, **108**, 13265-13272.
9 O. P. Varnavski, M. Ranasinghe, X. Yan, C. A. Bauer, S.-J. Chung, J. W. Perry, S. R. Marder and T. Goodson III, *J. Am. Chem. Soc.*, 2006, **128**, 10988-10989.
10 L. Shang, C. Qin, T. Wang, M. Wang, L. Wang and S. Dong, *J. Phys. Chem. C*, 2007, **111**, 13414-13417.
11 J. Griffin, A. K. Singh, D. Senapati, P. Rhodes, K. Mitchell, B. Robsinson, E. Yu and P. C. Ray, *Chem. Eur. J.*, 2009, **15**, 342-351.
12 J. Zhang, Y. Fu and J. R. Lakowicz, *J. Phys. Chem. C*, 2006, **111**, 50-56.
13 P. Anger, P. Bharadwaj and L. Novotny, *Phys. Rev. Lett.*, 2006, **96**, 113002/113001-4.
14 S. Kuhn, G. Mori, M. Agio and V. Sandoghdar, *Mol. Phys.*, 2008, **106**, 893-908.
15 J. Seelig, K. Leslie, A. Renn, S. Kuehn, V. Jacobsen, M. Van de Corput, C. Wyman and V. Sandoghdar, *Nano Lett.*, 2007, **7**, 685-689.
16 A. D'Aléo, R. M. Williams, Y. Chriqui, V. M. Iyer, P. Belser, F. Vergeer, V. Ruiz, P. R. Unwin and L. De Cola, *Open Inorg. Chem. J.*, 2007, **1**, 26-36.
17 M. H. V. Werts, H. Zaim and M. Blanchard-Desce, *Photochem. Photobiol. Sci.*, 2004, **3**, 29-32.
18 N. Nerambourg, Werts, M. Charlot and M. Blanchard-Desce, *Langmuir*, 2007, **23**, 5563-5570.
19 G. g. Schneider, G. Decher, N. Nerambourg, R. s. Praho, M. H. V. Werts and M. Blanchard-Desce, *Nano Lett.*, 2006, **6**, 530-536.
20 T. Gu, J. K. Whitesell and M. A. Fox, *Chem. Mater.*, 2003, **15**, 1358-1366.
21 T. L. Jennings, M. P. Singh and G. F. Strouse, *J. Am. Chem. Soc.*, 2006, **128**, 5462-5467.
22 J. van Herrikhuyzen, R. A. J. Janssen, A. P. H. J. Schenning and S. C. J. Meskers, *Chem. Phys. Lett.*, 2007, **433**, 340-344.
23 B. I. Ipe, K. G. Thomas, S. Barazzouk, S. Hotchandani and P. V. Kamat, *J. Phys. Chem. B*, 2002, **106**, 18-21.
24 A. Kotiaho, R. Lahtinen, H. Lehtivuori, N. V. Tkachenko and H. Lemmetyinen, *J. Phys. Chem. C*, 2008, **112**, 10316-10322.
25 A. Kotiaho, R. M. Lahtinen, N. V. Tkachenko, A. Efirnov, A. Kira, H. Imahori and H. Lemmetyinen, *Langmuir*, 2007, **23**, 13117-13125.
26 T. Wang, D. Zhang, W. Xu, J. Yang, R. Han and D. Zhu, *Langmuir*, 2002, **18**, 1840-1848.

27 I. Cohanoschi, S. Yao, K. D. Belfield and F. E. Hernandez, *J. Appl. Phys.*, 2007, **101**, 086112/086111-3.
28 W. Wenseleers, F. Stellacci, T. Meyer-Friedrichsen, T. Mangel, C. A. Bauer, S. J. K. Pond, S. R. Marder and J. W. Perry, *J. Phys. Chem. B*, 2002, **106**, 6853-6863.
29 L. Shang, C. Qin, T. Wang, M. Wang, L. Wang and S. Dong, *J. Phys. Chem. C*, 2007, **111**, 13414-13417.
30 J. Griffin, A. K. Singh, D. Senapati, P. Rhodes, K. Mitchell, B. Robinson, E. Yu and P. C. Ray, *Chem. Eur. J.*, 2009, **15**, 342-351.
31 S.-S. Kim, S.-I. Na, J. Jo, D.-Y. Kim and Y.-C. Nah, *Appl. Phys. Lett.*, 2008, **93**, 073307.
32 S. Gunes, H. Neugebauer and N. S. Sariciftci, *Chem. Rev.*, 2007, **107**, 1324-1338.
33 R. L. Sutherland, *Handbook of Nonlinear Optics*, Marcel Dekker, Inc., New York, 2003.
34 T. Soller, M. Ringler, M. Wunderlich, T. A. Klar, J. Feldmann, H. P. Josel, Y. Markert, A. Nichtl and K. Kuerzinger, *Nano Lett.*, 2007, **7**, 1941-1946.
35 C. Scharf, K. Peter, P. Bauer, C. Jung, M. Thelakkat and J. Köhler, *Chem. Phys.*, 2006, **328**, 403-409.
36 R. D. Hreha, C. P. George, A. Haldi, B. Domercq, M. Malagoli, S. Barlow, J.-L. Brédas, B. Kippelen and S. R. Marder, *Adv. Funct. Mater.*, 2003, **13**, 967-973.
37 A. B. Pangborn, M. A. Giardello, R. H. Grubbs, R. K. Rosen and F. J. Timmers, *Organometallics*, 1996, **15**, 1518-1520.
38 D. D. Perrin and L. F. Armarego, *Purification of Laboratory Chemicals*, Butterworth-Heinemann, Oxford, 1988.
39 S. L. Logunov, T. S. Ahmadi, M. A. El-Sayed, J. T. Khoury and R. L. Whetten, *J. Phys. Chem. B*, 1997, **101**, 3713-3719.
40 D. V. Leff, L. Brandt and J. R. Heath, *Langmuir*, 1996, **12**, 4723-4730.
41 H. L. Zhang, S. D. Evans, J. R. Henderson, R. E. Miles and T. Shen, *J. Phys. Chem. B*, 2003, **107**, 6087-6095.
42 M. Brust, M. Walker, D. Bethell, D. J. Schiffrin and R. Whyman, *J. Chem. Soc., Chem. Commun.*, 1994, 801-802.
43 A. Badia, L. Cuccia, L. Demers, F. Morin and R. B. Lennox, *J. Am. Chem. Soc.*, 1997, **119**, 2682-2692.
44 M. J. Hostetler, J. J. Stokes and R. W. Murray, *Langmuir*, 1996, **12**, 3604-3612.
45 A. Badia, S. Singh, L. Demers, L. Cuccia, G. R. Brown and R. B. Lennox, *Chem. Eur. J.*, 1996, **2**, 359-363.
46 R. G. Snyder, H. L. Strauss and C. A. Elliger, *J. Phys. Chem.*, 1982, **86**, 5145-5150.
47 R. G. Snyder, M. Maroncelli, H. L. Strauss and V. M. Hallmark, *J. Phys. Chem.*, 1986, **90**, 5623-5630.
48 M. D. Porter, T. B. Bright, D. L. Allara and C. E. D. Chidsey, *J. Am. Chem. Soc.*, 1987, **109**, 3559-3568.
49 P. E. Laibinis, R. G. Nuzzo and G. M. Whitesides, *J. Phys. Chem.*, 1992, **96**, 5097-5105.
50 R. M. Silverstein and F. X. Webster, *Spectrometric Identification of Organic Compounds*, John Wiley & Sons, Inc., New York, 1998.
51 M. J. Hostetler, J. E. Wingate, C. J. Zhong, J. E. Harris, R. W. Vachet, M. R. Clark, J. D. Londono, S. J. Green, J. J. Stokes, G. D. Wignall, G. L. Glish, M. D. Porter, N. D. Evans and R. W. Murray, *Langmuir*, 1998, **14**, 17-30.
52 G. C. Lica, B. S. Zelakiewicz and Y. Y. Tong, *J. Electroanal. Chem.*, 2003, **554-555**, 127-132.

53 A. D'Aléo, R. M. Williams, F. Osswald, P. Edamana, U. Hahn, J. van Heyst, F. D. Tichelaar, F. Vögtle and L. De Cola, *Adv. Funct. Mater.*, 2004, **14**, 1167-1177.
54 A. Badia, W. Gao, S. Singh, L. Demers, L. Cuccia and L. Reven, *Langmuir*, 1996, **12**, 1262-1269.
55 O. Kohlmann, W. E. Steinmetz, X.-A. Mao, W. P. Wuelfing, A. C. Templeton, R. W. Murray and C. S. Johnson, *J. Phys. Chem. B*, 2001, **105**, 8801-8809.
56 A. Badia, L. Demers, L. Dickinson, F. G. Morin, R. B. Lennox and L. Reven, *J. Am. Chem. Soc.*, 1997, **119**, 11104-11105.
57 R. H. Terrill, T. A. Postlethwaite, C.-h. Chen, C.-D. Poon, A. Terzis, A. Chen, J. E. Hutchison, M. R. Clark and G. Wignall, *J. Am. Chem. Soc.*, 1995, **117**, 12537-12548.
58 A. C. Templeton, J. J. Pietron, R. W. Murray and P. Mulvaney, *J. Phys. Chem. B*, 2000, **104**, 564-570.
59 G. Lanzani, S. V. Frolov, P. A. Lane, Z. V. Vardeny, M. Nisoli and S. De Silvestri, *Phys. Rev. Lett.*, 1997, **79**, 3066-3069.
60 Z. Wang, S. Mazumdar and A. Shukla, *Phys. Rev. B*, 2008, **78**, 235109.
61 T. Tsuboi, A. K. Bansal and A. Penzkofer, *Opt. Mater.*, 2009, **31**, 980-988.
62 M. A. Loi, A. Mura, G. Bongiovanni, Q. Cai, C. Martin, H. R. Chandrasekhar, M. Chandrasekhar, W. Graupner and F. Garnier, *Phys. Rev. Lett.*, 2001, **86**, 732-735.
63 M. Wolffs, N. Delsuc, D. Veldman, N. Van Anh, R. M. Williams, S. C. J. Meskers, R. A. J. Janssen, I. Huc and A. P. H. J. Schenning, *J. Am. Chem. Soc.*, 2009, **131**, 4819-4829.
64 A. Sautter, B. K. Kaletas, D. G. Schmid, R. Dobrawa, M. Zimine, G. Jung, I. H. M. van Stokkum, L. De Cola, R. M. Williams and F. Wurthner, *J. Am. Chem. Soc.*, 2005, **127**, 6719-6729.
65 N. Van Anh, F. Schlosser, M. M. Groeneveld, I. H. M. van Stokkum, F. Würthner and R. M. Williams, *J. Phys. Chem. C*, 2009, **113**, 18358-18368.